# Investigation of bistable switching in linear tapered nonlinear Bragg gratings

JIAN-FENG TIAN*
*Department of Physics, Taiyuan Normal University, Taiyuan 030031, China*

Based on the coupled mode theory, by using the time-domain transfer matrix method, the bistable performance and dynamic switching characteristics of linear tapered nonlinear Bragg gratings (LT-NLBG) are analyzed numerically. We consider both the positive and negative tapered case and compare their performance as a nonlinear switch. The results show that, With the quasi-continuous wave taken into consideration, for the various tapered factors, the temporal characteristics exists with significant difference, including output self-pulsation amplitude, time delay and pulse-width, etc.; As a short pulse switching device, the positive tapered gratings display much less splitting, an indication that modulation instability is not playing a significant role, and the transmitted pulse is much more intense than that in the negative tapered case.

(Received July 7, 2013; accepted May 15, 2014)

*Keywords:* Bragg gratings, Linear tapered, Bistable switching

## 1. Introduction

Compact all-optical switches and logic gates are of high interest in view of their applications in future packet switched networks. A leading candidate for such devices is the nonlinear Bragg grating which exhibits particular properties near the edge of "photonic band gap" (PBG). Outside PBG, slow Bragg soliton related to great anomalous group velocity dispersion (GVD) has been used for ultra-short optical pulse compression successfully [1-4]; Inside PBG, it shows bistable optical behavior with regard to the intensity of the input beam. The optical bistability has wide applications in optical signal processing, optical memory, optical limiting, optical switching and optical gate operations, etc [5-7]. Many efforts have been made to offer additional feasibility of NLBG, such as the switching-on threshold, the switching time, the on-off switching ratio and dynamic stability, etc. The used technologies mainly include spatial taper, phase shift, chirp and nonlinear refractive index axial varying, etc [8-12]. For the LT-NLBG gratings, earlier studies mostly were mainly carried out under the continuous wave (CW) hypothesis [8, 9], but it is essential to study its dynamic properties since the self-pulsing and chaos may happen in the upper branch of hysteresis due to modulation instability (MI) [13,14].

In this paper, the bistable steady characteristics and dynamic switching characteristics of LT-NLBG have been analyzed based on the nonlinearly coupled mode equations (NLCME). The numerical simulations show that, depending upon the various tapered factors, the switching behavior is different both in stable and temporal characteristics. In the following we will discuss them separately, and the underlined mechanism is analyzed.

## 2. Theoretical model

Inside fiber gratings, the $z$ -axial distribution of refractive index can be described by

$$n(z) = n_0 + n_1(z)\cos\left[2\beta_B(z)z + \Omega(z)\right] + n_2\left|E(z)\right|^2, \quad (1)$$

where $E(z)$ is the inner electric field of gratings, $\beta_B(z)$ is the Bragg wave vector, $\Omega(z)$ is the spatial phase shift. $n_0$, $n_1(z)$ and $n_2$ denote the effective mode refractive index, linear refractive index modulation amplitude, and nonlinear refractive index coefficient, respectively.

The inner electric field can be expressed by

$$E(z) = E_+(z)\exp\{i[\beta_B(z)z - \omega t]\} + E_-(z)\exp\{-i[\beta_B(z)z + \omega t]\} \quad (2)$$

where $\omega$ is the carrier angular frequency, $t$ is the

time, $E_+$ and $E_-$ represent the slowly varying amplitude of forward and backward wave, respectively. Substituting Eqs. (1) and (2) into the wave equations, and neglecting the loss and material dispersion(the nonlinear medium of NLBG is assumed to be Erbium-doped fiber without pump, even though its loss and material dispersion coefficients near $1.55\mu m$ are large, the total loss and material dispersion are negligible due to very short length selected in calculations), the response time of material is very fast enough, as well as the carrier wavelength is close to Bragg wavelength, one can obtain the following nonlinear coupled mode equations [2]

$$\frac{\partial E_+}{\partial z}+\frac{1}{v_g}\frac{\partial E_+}{\partial t}=i[\delta E_+ +\gamma(|E_+|^2+2|E_-|^2)E_+ +kE_-], \quad (3a)$$

$$-\frac{\partial E_-}{\partial z}+\frac{1}{v_g}\frac{\partial E_-}{\partial t}=i[\delta E_- +\gamma(|E_-|^2+2|E_+|^2)E_+ +kE_+], \quad (3b)$$

where $v_g$ is the light group velocity in the grating medium, $\delta$, $\gamma$ and $k$ account for the detuning from the Bragg vector, nonlinear coefficient, and coupling coefficient, respectively, which can be expressed by

$$\delta=\beta-\beta_B(z)=n_0\frac{\omega}{c}-\beta_B(z),$$

$$\gamma=\frac{\pi n_2}{\lambda_B},$$

$$k=\frac{\pi n_1(z)}{\lambda_B}, \quad (4)$$

where $c$ is the light velocity in vacuum, $\lambda_B=2n_0\Lambda$ is the Bragg wavelength, $\Lambda$ is the grating period,

For linear tapered NLBG, $k$ can be written as [8]

$$k(z)=k_0[1+\Delta k(z-L/2)/L] \quad (5)$$

where $L$ is the total length of grating, $k_0$ is the coupling coefficient of the grating center, and $\Delta k$ characterizes the variation slop of coupling coefficient, Its positive(negative) value corresponds to the positive(negative) tapered.

The boundary conditions are given by

$$z=0:\ E_+(0,t)=E_i(0,t),\ E_r(0,t)=E_-(0,t), \quad (6a)$$

$$z=L: E_-(L,t)=0, E_t(L,t)=E_+(L,t), \quad (6b)$$

where $E_i$, $E_r$ and $E_t$ are the slowly varying amplitudes of the incident, reflected and transmitted wave, respectively.

Setting the spatial derivative with respect to $t$ in Eqs. (3a) and (3b) equal to zeros, the axial evolving equations of slowly varying amplitude under steady-state can be analyzed numerically by means of the fourth-order Runge-Kutta method together with boundary conditions.

To simulate the output dynamics characteristics, the modified time-domain transfer-matrix method(TMM) can be utilized [14]. Split the length $L$ into $M$ equal sections from input end, assume each section is uniform, and label the localized amplitudes before and after each section as $E_{+j}(E_{-j})$ and $E_{+(j+1)}(E_{-(j+1)})$ (j=1,2,…..M), respectively, then

$$\begin{bmatrix}E_{+,j+1}(t+\Delta t)\\ E_{-,j}(t+\Delta t)\end{bmatrix}=T_pT_c\begin{bmatrix}E_{+,j}(t)\\ E_{-,j+1}(t)\end{bmatrix}, \quad (7a)$$

where the time step size $\Delta t$ is related to spatial step size $\Delta z$ as $\Delta t=\Delta z/v_g'$, the matrixes $T_c$ and $T_p$ respectively denote the coupling and detuning terms, given by

$$T_c=\begin{bmatrix}\sec h(k\Delta z) & i\tanh(k\Delta z)\\ i\tanh(k\Delta z) & \sec h(k\Delta z)\end{bmatrix} \quad (7b)$$

$$T_p=\begin{bmatrix}\exp\left\{i\Delta z\left[\delta+\gamma(|E_{+,j}(t)|^2+2|E_{-,j}(t)|^2)\right]\right\} & 0\\ 0 & \exp\left\{i\Delta z\left[\delta+\gamma(|E_{-,j+1}(t)|^2+2|E_{+,j+1}(t)|^2)\right]\right\}\end{bmatrix} \quad (7c)$$

Start from the boundary condition (6b), calculating iteratively the Esq. (7a)-(7b), together with the boundary condition (6a), one can obtain the whole output wave of the nonuniform fiber grating.

## 3. Results and discussion

The used data in calculations are $\lambda_B = 1.55\mu m$ , $n_2 = 2.5\times10^{-15} m^2/w$ , $L = 1cm$ , $k_0 = 5cm^{-1}, \delta L = 3$. To facilitate description, the input light powers $P_i$, and the output powers $P_t$ are normalized as $P_i / P_c$ and $P_t / P_c$ respectively in following discussions, where $P_c = 4\lambda_B A_{eff} / 3\pi n_2 L$ is the critical input power, and $A_{eff} = 0.4\mu m^2$ is the effective area of waveguide [9].

### a) Bistability performance analysis

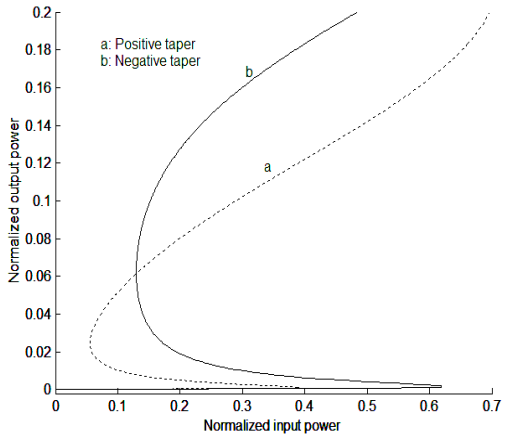


*Fig. 1. Input-output characteristics curves for LT-NLBG.*

Fig. 1 shows the steady-state input-output characteristics curves for LT-NLBG, where $|\Delta k| = 30\%$. From Fig. 1, it can be seen that, comparing positive tapered, negative tapered-NLBG increases the switching-on threshold, the width of the hysteresis and the on-off switching ratio significantly. The taper-dependent bistability is due to the difference of the axial distribution of forward wave intensity in the gratings [8].

### b) Quasi-CW switching characteristics

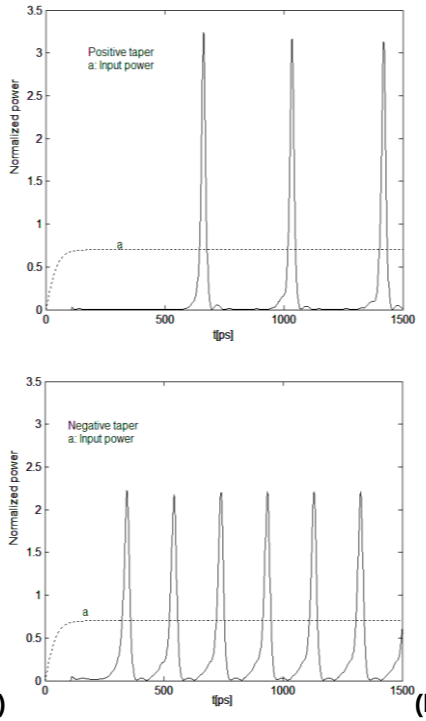


*Fig. 2. Normalized input-output powers for LT-NLBG, $\Delta k$ is (a) 30% and (b) -30%.*

To understand the instability of the upper state in Fig. 1, we consider the continuous wave (CW) limit by using an input field whose intensity rises quickly (rise time ~100ps) and then settles down a constant value. The dotted line in Fig. 2 shows the input power profile, and Fig. 2 shows normalized output powers for LT-NLBG, where $P_i / P_c = 0.7$ , $\Delta k$ is (a) 30% and (b) -30%. From Fig. 2 (a) and (b), one can see that, with the CW taken into consideration, the periodic self-pulsation may emerge extremely easy under the dynamic conditions in NLBG, and comparing negative tapered case, the positive tapered NLBG output self-pulsation wave has greater delay time, the output pulse width is narrower, and pulse sequence base is smaller, but the amplitude of self-pulsation increase.

The oscillation of the output light can be interpreted as modulation instability, which is a result of an interplaying between the nonlinear and dispersive effects. The periodic structure provides a very large anomalous group velocity dispersion near the upper edge of the stop gap. When the incident power above the threshold, the

steady-state propagation of the CW is inherently unstable, new frequency wave will be generated, which can be explained in terms of four-wave mixing phase-matched.

### c) Short pulse switching characteristics

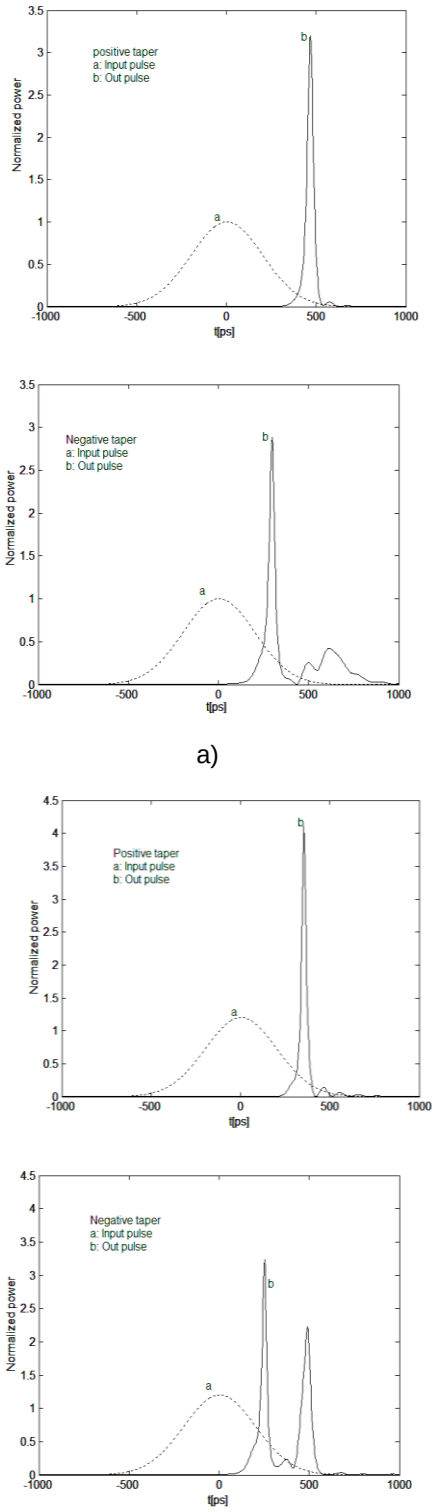


*Fig. 3. Input and output pulse shapes for LT-NLBG, the normalized input peak power is (a) 1.0 and (b) 1.2.*

Fig. 3 the input and output pulse shapes for LT-NLBG, where $|\Delta k| = 30\%$ , and the normalized input peak power $P_i / P_c$ is (a) 1.0 and (b) 1.2. The input peak power is selected above the threshold according to Fig. 1. The input pulse is assumed to be Gaussian shape with 200ps width. For positive tapered case, we observe much less splitting, an indication that modulation instability is not playing a significant role, and the transmitted pulse is much more intense than that in the negative tapered case. In fact, the narrowed transmitted pulse for positive-tapered NLBG is a Bragg soliton. From the physical point of view, the Bragg soliton comes from the balance of anomalous group velocity dispersion near PBG and self-phase modulation (SPM). For input pulse with larger peak power [see Fig. 3(b)], the normalized peak power of transmitted Bragg soliton is further increased up to ~2.2 owing to the enhanced SPM.

## 4. Conclusions

In summary, we have investigated numerically the bistable performance and dynamic switching characteristics of linear tapered nonlinear Bragg gratings. We considered both the positive and negative taper case and compared their performance as a nonlinear switch. The nonlinear coupled-mode equations were solved numerically to obtain switching characteristics. The results show that, With the quasi-continuous wave taken into consideration, for the various tapered factors, the temporal characteristics exists with significant difference, including output self-pulsation amplitude, time delay and pulse-width, etc., the modulation instability is responsible for the instability; As a short pulse switching device, the positive tapered gratings display much less splitting, an indication that modulation instability is not playing a significant role, and the transmitted pulse is much more intense than that in the negative tapered case; For the negative tapered gratings, the shape of the transmitted pulses can change dramatically from that of the input pulse, especially when pulse peak power is large. Despite this paper deals only with switching characteristics analysis for NLBG with cosine refractive index modulation, further study shows that, for arbitrary nonlinear periodic structures, the influence of the linear tapered on its dynamic performance exhibits similar behaviors.

## Acknowledgement

The author acknowledges the support by the Special Foundation for Shanxi Province Universities Science and Technology Development of the People's Republic of China (Grant Number 20121110).

## References

[1] I. V. Kabakova, C. M. de Sterke, B. J. Eggleton, J. Opt. Soc. Am. B, **27**(12), 2648 (2010).
[2] B. J. Eggleton, G. Lenz, N. M. Litchinitser, Fiber and Integrated Opt. **19**(4), 383 (2000).
[3] N. G. R. Broderick, P. Millar, D. J. Richardson, J. S. Aitchson, R. De La Rue, T. Krauss, Opt. Lett., **25** (10), 740 (2000).
[4] H. G. Winful, J. H. Marburger, E. Garmire, Appl. Phys. Lett., **35**(5), 379 (1979).
[5] N. G. R. Broderick, D. Taverner, D. J. Richardson, Opt. Express, **3**(11), 447 (1998).
[6] N. Peyghambarian, H. M. Gibbs, J. Opt. Soc. Am. B, **2**(7), 1215 (1985).
[7] L. Brzozowski, E. H. Sargent, IEEE J. Quantum Electron., **36**(5), 550 (2000).
[8] X. H. Jia, Z. M. Wu, G. Q. Xia, Opt. express, **12**(13), 2945 (2004).
[9] A. Maitra, C. G. Poulton, J. Wang et al., IEEE J. Quantum Electron., **41**(10), 1303 (2005).
[10] J. F. Tian, Optik, **122**(15), 1381(2011).
[11] G. P. Agrawal, S. Radic, IEEE Photon. Technol. Lett., **6**(8), 995 (1994).
[12] H. Lee, G. P. Agrawal, IEEE J. Quantum Electron., **39**(3), 508 (2003).
[13] F. Marquis, P. Dobiasch, P. Meystre, E. M. Wright, J. Opt. Soc. Am. B, **3**(1), 50 (1986).
[14] B. S. Kim, Y. Chung, J. S. Lee, IEEE J. Quantum Electron., **36**(7), 787 (2000).

*Corresponding author: jianfeng2000@aliyun.com